Electronic Supplementary Information (ESI)

Urethral reconstruction using an amphiphilic tissue-engineered autologous polyurethane nanofibers scaffold with rapid vascularized function

Yuqing Niu[a, b], *Guochang Liu*[d], *Chuangbi Chen*[b], *Ming Fu*[d], *Wen Fu*[d], *Zhang Zhao*[d], *Huimin Xia*[a, d,*], *Florian J. Stadler*[b,*]

[a.] Department of Pediatric Surgery, Guangzhou Institute of Pediatrics, Guangzhou Women and Children's Medical Center, Guangzhou Medical University, Guangzhou 510623, Guangdong, China

[b.] Nanshan District Key Lab for Biopolymers and Safety Evaluation, Shenzhen Key Laboratory of Polymer Science and Technology, Guangdong Research Center for Interfacial Engineering of Functional Materials, College of Materials Science and Engineering, Shenzhen University, Shenzhen 518055, PR China

[c.] State Key Laboratory of Virology, Wuhan Institute of Virology, Chinese Academy of Sciences, Wuhan, 430071 China

[d.] Department of Pediatric Urology, Guangzhou Women and Children's Medical Center, Guangzhou Medical University, Guangzhou 510623, Guangdong, China.

Materials characterizations

1.1 NMR spectroscopy. ^{1}H NMR spectra were recorded at room temperature in D-chloroform ($CDCl_3$) at a concentration of 20 mg/mL on a Bruker AV 400 NMR spectrometer to determine the chemical structure of the copolymers. Tetramethylsilane was used as the internal standard.

1.2 Thermal analysis. Differential scanning calorimetry (DSC) was performed on TA Instruments Q100 and Q50 respectively under nitrogen atmospheres. The DSC analysis was as following: a sample of 2.5 mg in an aluminum pan was cooled from room temperature to -60 ℃ by an auto cool accessory, the pan was heated from -60 ℃ to 180 ℃ at a 10 ℃ /min rate, isothermally maintained at 180

℃ for 3 min, quenched to -60 ℃, and reheated from -60 ℃ to 180 ℃ at 10 ℃/min under a nitrogen flow rate of 50 mL/min. Data were collected during the second heating run. The glass-transition temperature (T_g) was taken as the midpoint of the heat capacity change. Melting point (T_m) was taken as the summit of melting peak and melting enthalpy (ΔH_m) was calculated from the area of the endothermic peak.

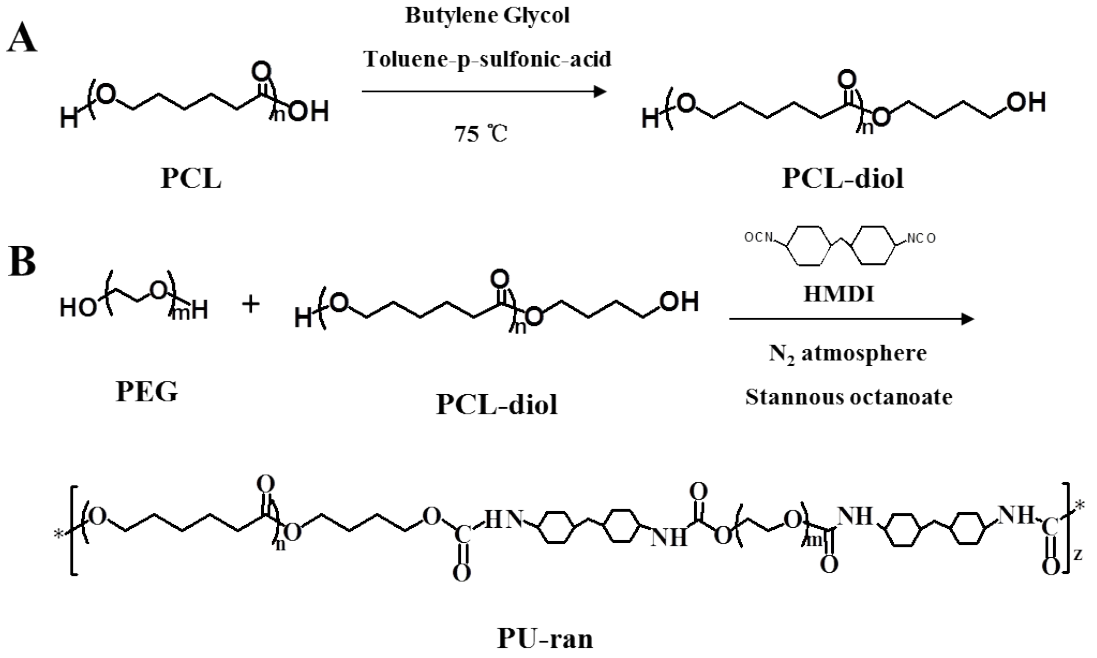

Fig.S1 Synthesis scheme of amphiphilic PU-ran based on PCL-diol and PEG. (A) Preparation of PCL-diol with dihydroxyl terminals; (B) The amphiphilic block PU-ran copolymers containing PCL-diol and PEG in soft segments and HMDI in hard segments were prepared.

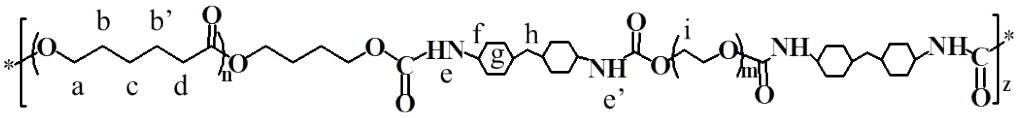

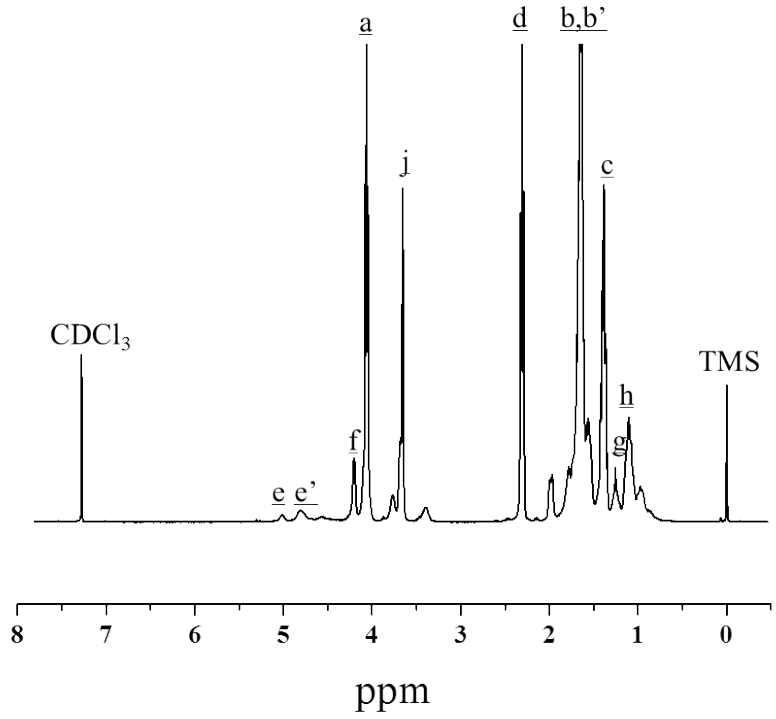

Fig.S2 ^{1}H NMR spectrum of PU-ran (E10-ran-C20) in $CDCl_3$.

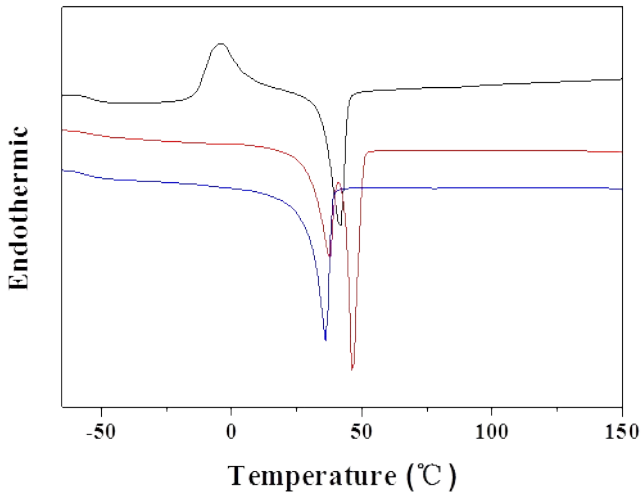

Fig.S3 DSC thermograms (2nd heating run) of PU-ran copolymers (10 °C/min).

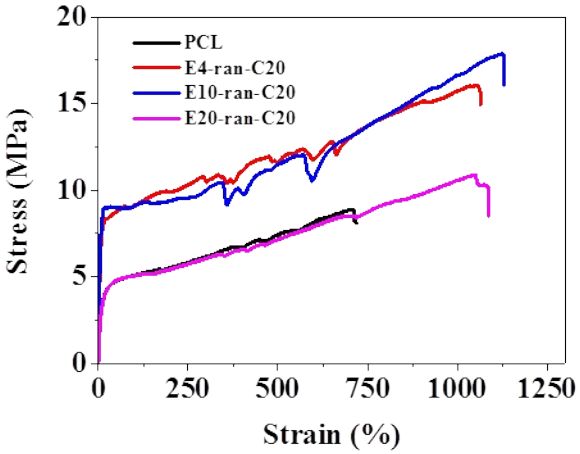

Fig.S4 Stress-strain curve of PCL, E4-ran-C20, E10-ran-C20, and E20-ran-C20 nanofiber scaffolds under wet conditions.

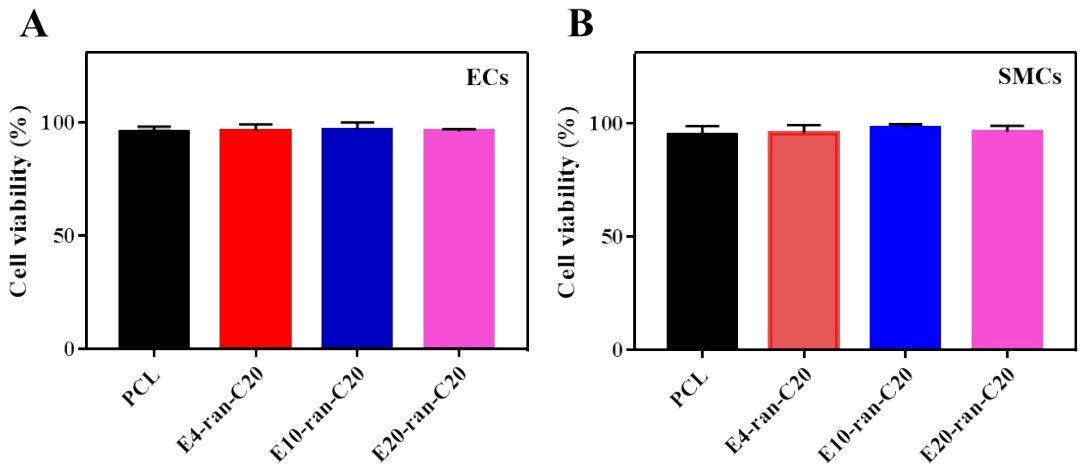

Fig. S5 Cell viability of (A) ECs and (B) SMCs after incubation with different nanofiber films at 37 °C for 72 h, as determined by using CCK-8 assay (*n*=3). Data are shown as mean ± s.e.m.

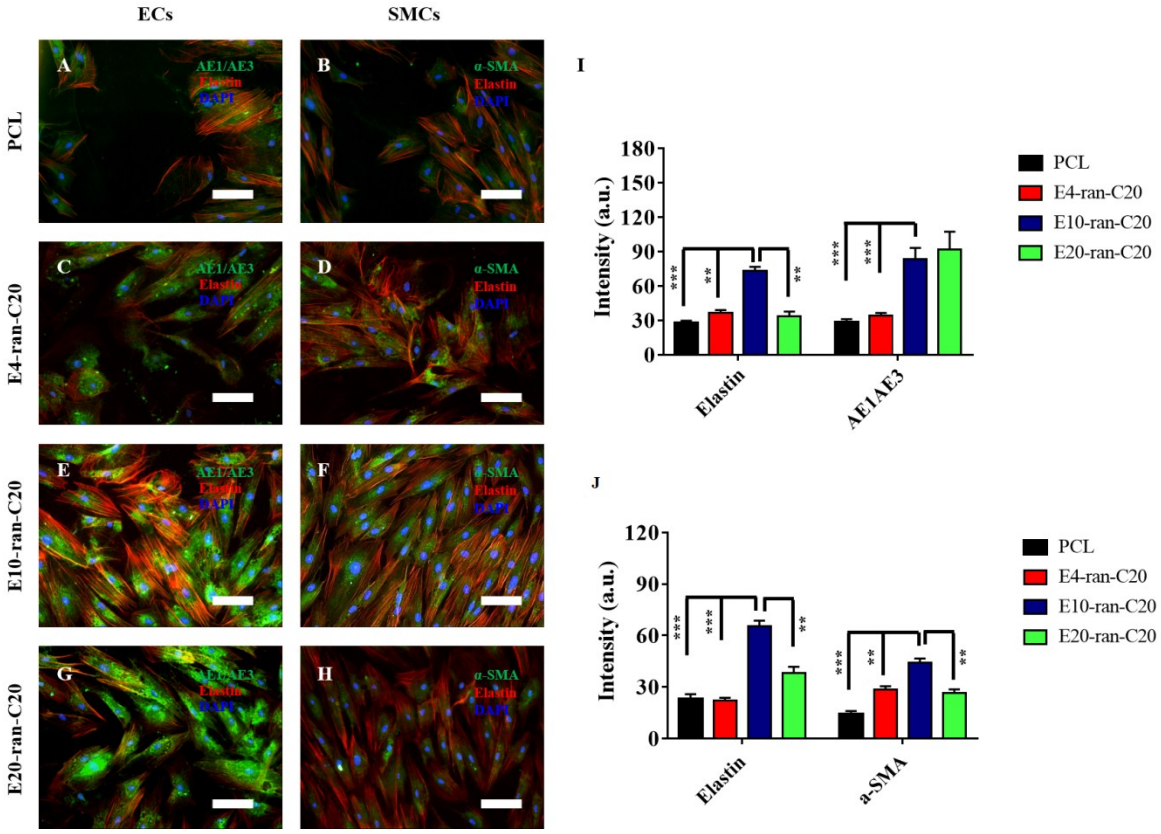

Fig.S6 ***In vitro*** **cell phenotypic expression and matrix synthesis.** Immunocytochemical analysis of the protein expression of (A, C, E, G) AE1/AE3 (green staining) of ECs, and (B, D, F, H) α-SMA (green staining) of SMCs as well as their respective elastin (red staining) on different substrates at 72 hours of cultivation. Scale bars, 60 μm. Quantification of the averaged (I) AE1/AE3+/Elastin+ in ECs and (J) SMA+/Elastin+ in SMCson different substrates (n=3, ANOVA, **$p < 0.01$, ***$p < 0.001$).

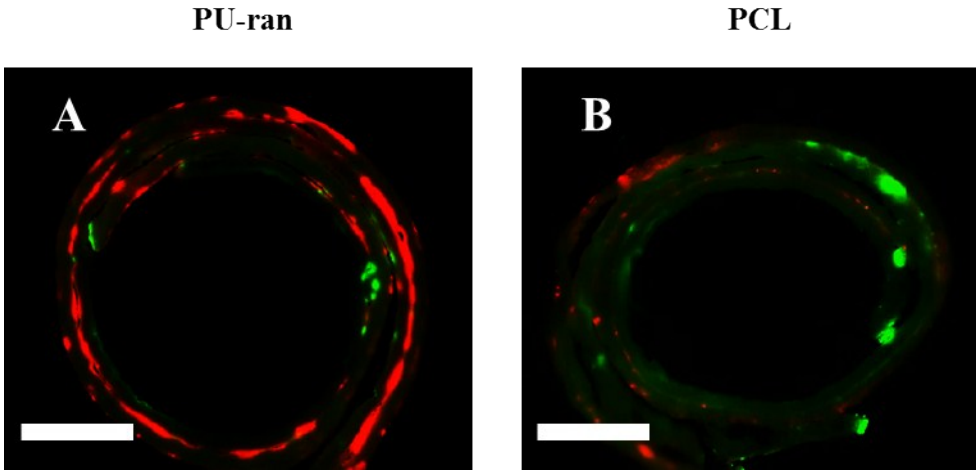

Fig.S7 Immunofluorescence analysis. CLSM images of cross section of tissue-engineered urethral scaffold based on (A) PU-ran and (B) PCL tubular scaffold. Scale bars, 1 mm.

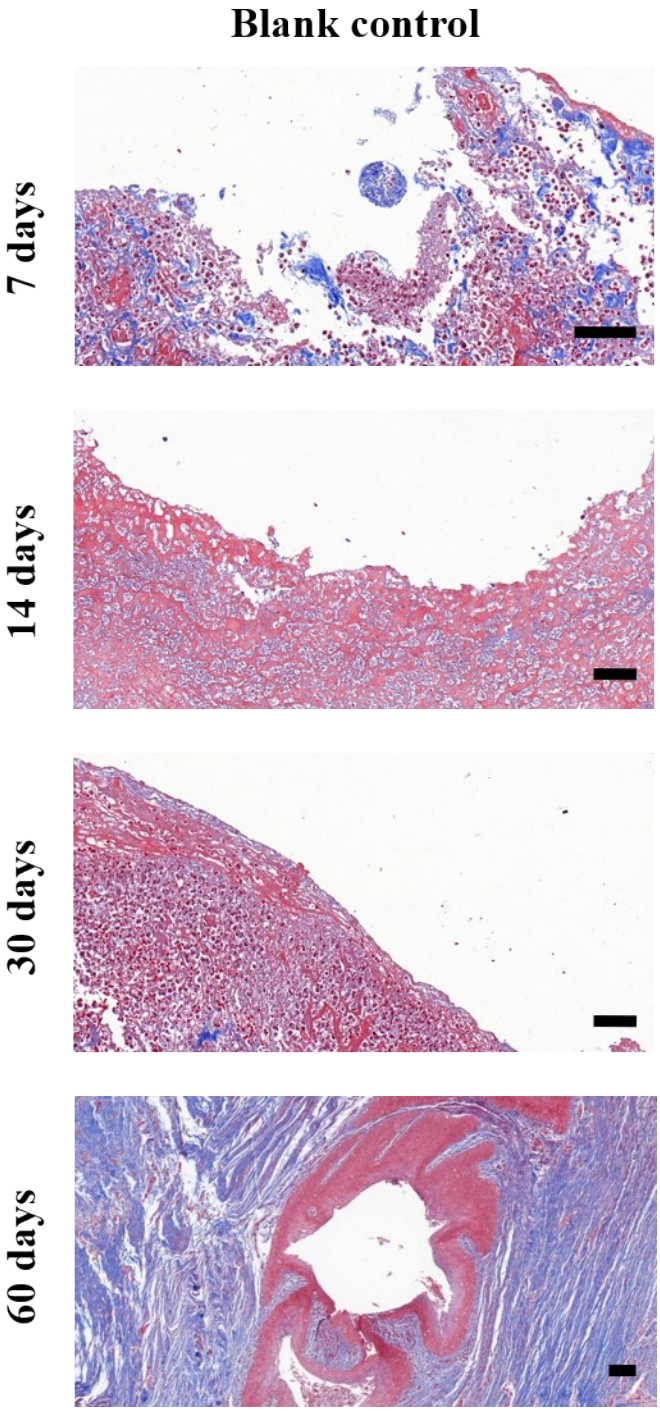

Fig. S8 Masson's trichrome staining of the cross-section of the mid-section of blank control group at the predetermined time points after implantation. Collagen (blue), smooth muscle (red). Scale bar, 50 μm.

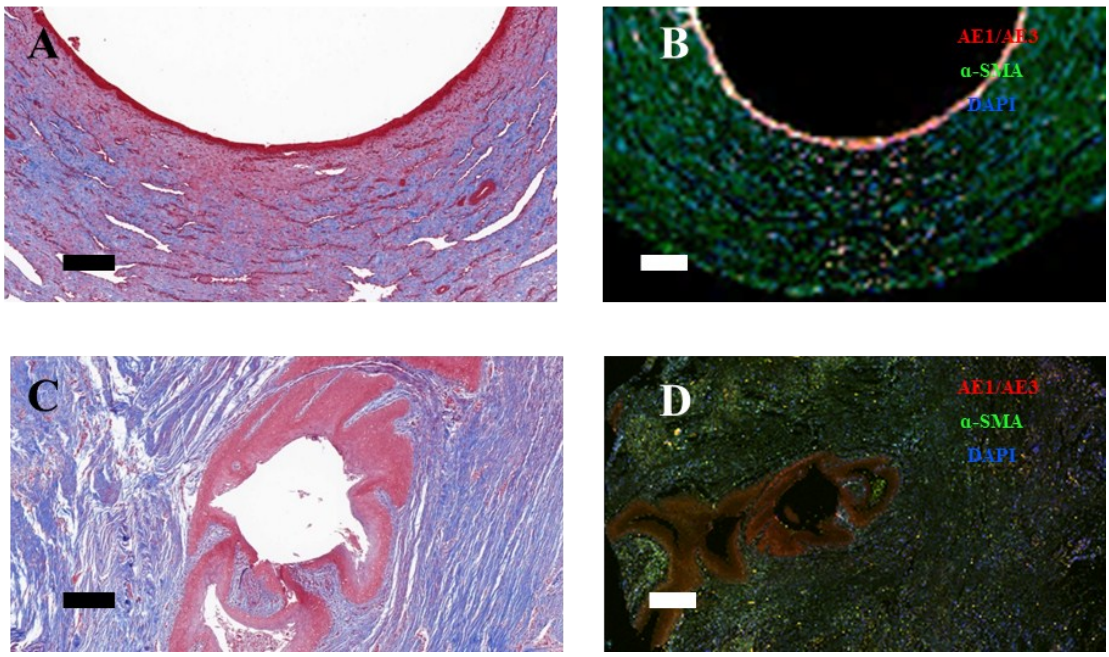

Fig.S9 Histological analysis of normal urethras and the injured urethras without scaffold. Masson's trichrome staining of the cross-section of (A) the normal beagle urethras and (C) the injured urethras at 10 ×. (B, D) Fluorescent staining of the same cross-section stained for epithelial tissue (red), smooth muscle tissue (green) and nuclei (blue) at 10 ×. (A-B) normal urethras, (C-D) injured urethras. Scale bars, 100 μm.

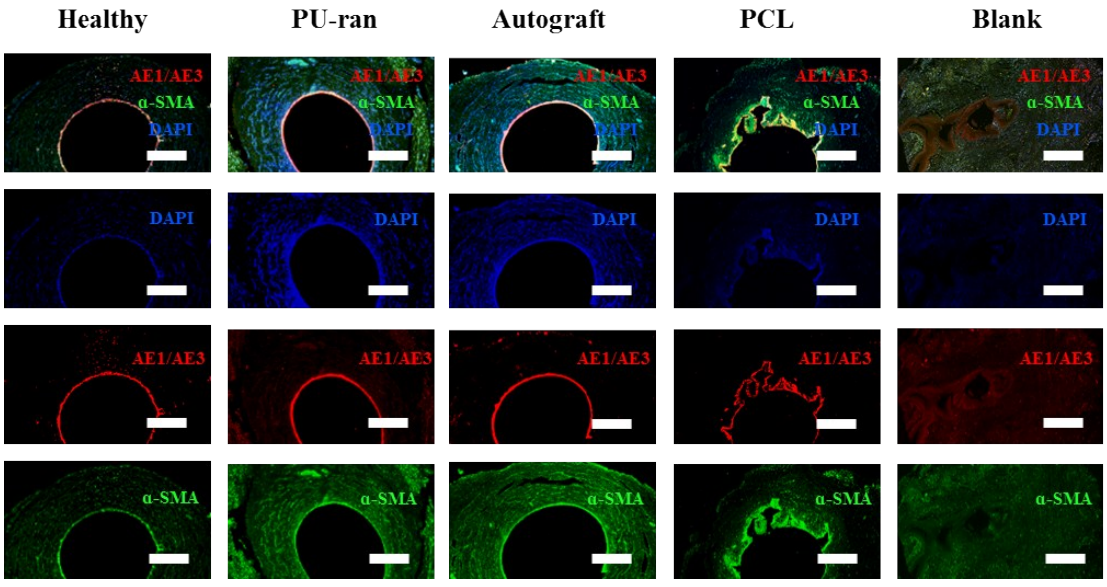

Fig.S10 Double-labeling immunofluorescence analysis. Compared with Healthy urethras, confocal laser scanning microscopy (CLSM) images of the mid-section of regenerated urethras after transplantation in each group at 60 days post-transplantation. Scale bars, 1 mm.

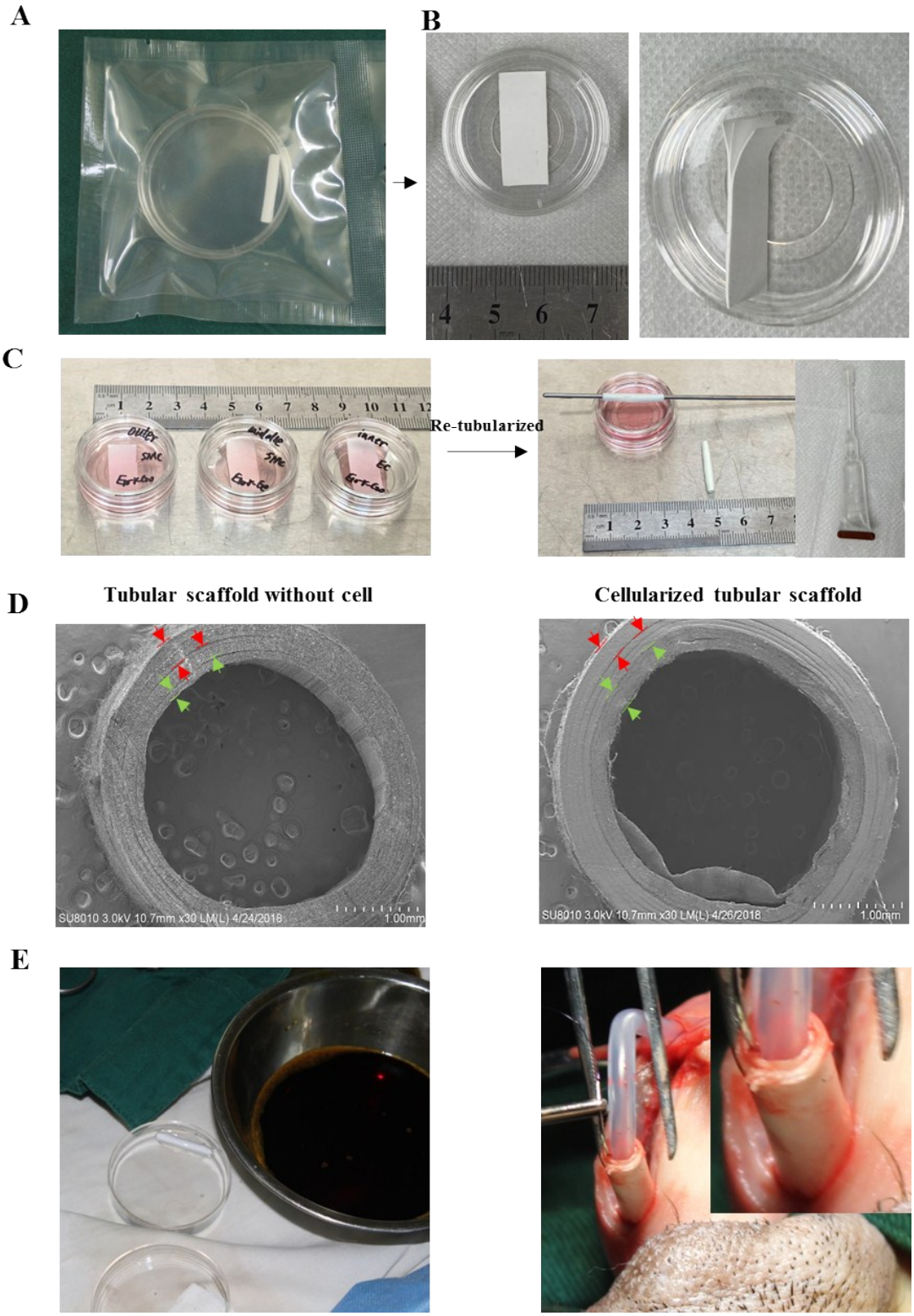

Fig.S11. Preparation of a cellularized PU-ran scaffold for transplantation. (A) The stratified tubular PU-ran (E10-ran-C20) nanofiber scaffolds were prepared by electrospinning and then packaged in a cell culture dish after irradiation sterilization. (B) When cells are inoculated, the stratified tubular nanofiber scaffold was cut into nanofiber film along the long axis of cylindrical sterile stainless steel. Three concentric nanofiber films were generated. (C) After inoculating corresponding seeded cells on three concentric nanofiber films, the original concentric nanofiber films were wrapped on the sterile cylindrical stainless steel axis to form a cellularized stratified tubular PU-ran nanofiber scaffold. (D) SEM images of stratified tubular PU-ran (E10-ran-C20) nanofiber scaffolds before seeded cells seeding and after seeded cells seeding. (E) The cellularized stratified tubular PU-ran (E10-ran-C20) nanofiber scaffold was transplanted to the urethral defective site. Two red arrows indicate the outer layer, two green arrows indicate the inner layer, and one red and one green arrow indicate the middle layer.

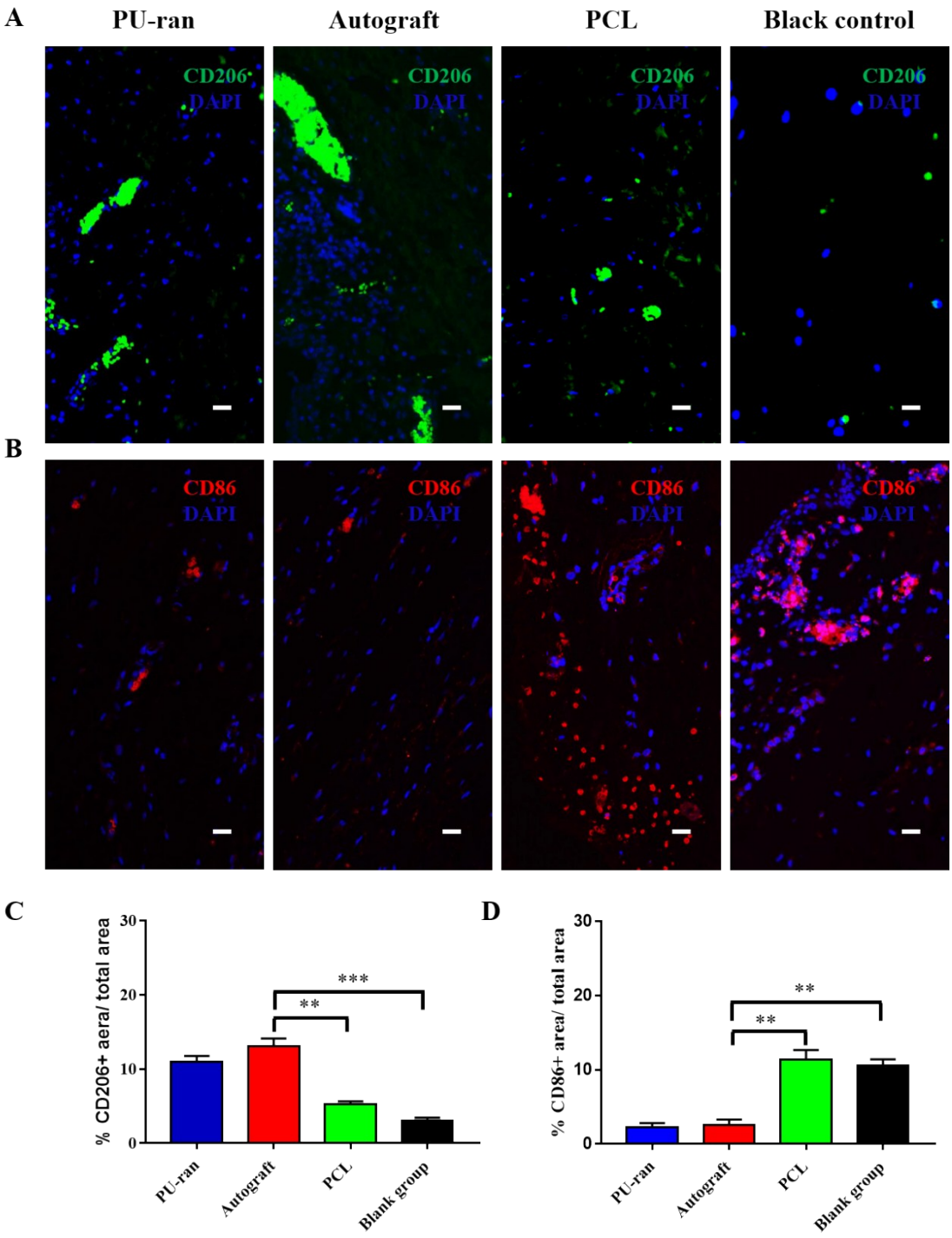

Fig. S12. Host macrophage response to scaffold at 30 days post-implantation. Fluorescent microphotos of the cross-section of the mid-section of each regenerated urethras stained for (A) CD206 (green), nuclei (blue) (A) and (B) CD86 (red), nuclei (blue) 30 days post transplantation. Scale bar, 30 μm. Quantification of the (C) constructive remodeling M2 (CD206+) macrophages and (D) pro-infammatory M1

(CD86+) macrophages in each regenerated urethras (n = 3, ANOVA, **p < 0.01, ***p < 0.001).

Table. S1 Mechanical properties of PCL and PU-ran copolymers in wet state.

Sample	R[a]	E (GPa)[b]	δ (MPa)[c]	ε (%)[d]
PCL	-	0.35 ± 0.07	12.5 ± 1.3	120-700
E4-ran-C20	1:2:1	1.78 ± 0.02	14.6 ± 0.5	190-1100
E10-ran-C20	1:2:1	1.82 ± 0.09	15.9 ± 0.8	200-1400
E20-ran-C20	1:2:1	0.6 ± 0.07	8.7 ± 0.6	130-950

a: PCL-diol/HMDI/PEG molar ratio in feed.

b: Young's modulus.

c: Stress at yield.

d: Strain at break.

Sample abbreviation E4-ran-C20 means that the feeding PEG segment M_n=0.4 kDa; PCL-diol segment M_n=2.8 kDa, and so on.

TableS2. Contact water angle of PCL and PU-ran copolymer nanofibers.

Materials	θH_2O (°)
PCL	119 ± 1.5
E4-ran-C20	92.7 ± 0.8
E10-ran-C20	80.5 ± 1.1
E20-ran-C20	48.9 ± 2.5